

Beam asymmetries in near threshold omega photoproduction off the proton

Frank Klein¹, A.V. Anisovich^{2,3}, J. C. S. Bacelar⁴, B. Bantes¹, O. Bartholomy², D. Bayadilov^{2,3}, R. Beck², Y.A. Beloglazov³, R. Castelijns⁴, V. Crede^{2,6}, H. Dutz¹, A. Ehmanns², D. Elsner¹, K. Essig², R. Ewald¹, I. Fabry², M. Fuchs², Ch. Funke², R. Gregor⁷, A. B. Gridnev³, E. Gutz², S. Höffgen¹, P. Hoffmeister², I. Horn², I. Jaegle⁵, J. Junkersfeld², H. Kalinowsky², S. Kammer¹, V. Kleber¹, Friedrich Klein¹, E. Klempt², M. Konrad¹, M. Kotulla^{5,7}, B. Krusche⁵, M. Lang², H. Löhner⁴, I.V. Lopatin³, J. Lotz², S. Lugert⁷, D. Menze¹, T. Mertens⁵, J.G. Messchendorp⁴, V. Metag⁷, C. Morales¹, M. Nanova⁷, V.A. Nikonov^{2,3}, D. Novinski^{2,3}, R. Novotny⁷, M. Ostrick¹, L.M. Pant⁷, H. van Pee^{2,7}, M. Pfeiffer⁷, A. Radkov³, A. Roy⁸, A.V. Sarantsev^{2,3}, S. Schadmand⁷, C. Schmidt², H. Schmieden^{1,*}, B. Schoch⁵, S.V. Shende⁴, V. Sokhoyan², A. Süle¹, V.V. Sumachev³, T. Szczepanek², U. Thoma^{2,7}, D. Trnka⁷, R. Varma⁷, D. Walther¹, Ch. Weinheimer², Ch. Wendel²

(The CBELSA/TAPS Collaboration)

¹*Physikalisches Institut, Universität Bonn, Germany*

²*Helmholtz-Institut für Strahlen- u. Kernphysik, Universität Bonn, Germany*

³*Petersburg Nuclear Physics Institute, Gatchina, Russia*

⁴*KVI, Groningen, The Netherlands*

⁵*Department Physik, Universität Basel, Switzerland*

⁶*Department of Physics, Florida State University, Tallahassee, USA*

⁷*II. Physikalisches Institut, Universität Gießen, Germany*

*

(Dated: October 30, 2018)

The photoproduction of ω mesons off protons has been studied at the Bonn ELSA accelerator from threshold to $E_\gamma = 1700$ MeV. Linearly polarized beams were produced via coherent bremsstrahlung. Large photon asymmetries in excess of 50% were obtained, whereas the pion asymmetries from $\omega \rightarrow \pi^0 \gamma$ are close to zero. The asymmetries do characteristically depend on Θ_{cm} rather than $|t|$ and indicate s-channel resonance formation on top of t-channel exchange processes.

PACS numbers: 13.60.Le, 13.88.+e, 14.40.Cs

The structure of the nucleon as viewed at very small distances is considered well understood in terms of pointlike, light quarks and gluons which mediate the mutual interaction. The mechanism of how the quarks are confined to form the nucleon, how basic properties such as mass and spin emerge in the strongly interacting system, is however only qualitatively understood [1].

The internal structure reflects itself in the excitation spectrum of the composite system which is related to the effective degrees of freedom. At the size scale of the nucleon those are expected to be dominantly hadronic in nature and the coupling of baryons and mesons to be important. Making use of the large interaction strength, pion-nucleon scattering provided the basis of the investigation of the nucleon excitation spectrum.

Its description in terms of the basic pointlike quarks and their gluonic interaction in the frame of Lattice-QCD is still in its infancy. Hence, quark models (which often attempt to incorporate basic QCD symmetries) provide an important guidance for our understanding. They all exhibit a general problem: Many more higher-lying states are predicted than experimentally observed. It was speculated that some excited states may decouple from the pion-nucleon channel and rather couple to non-

pionic channels [2]. The photoproduction of ω mesons off the proton is well suited to investigate this issue. It further benefits from the fact that the ω threshold is in the higher lying third resonance region of the nucleon. The narrow width of 8 MeV of the ω improves the signal to background ratio. In addition, the ω is isoscalar ($I = 0$); hence a s-channel process will only connect N^* ($I = 1/2$) states with the nucleon ground state, but no Δ^* with $I = 3/2$. This provides a great simplification to the complexity of the contributing excitation spectrum.

However, achieving a complete set of observables with respect to the decomposition of the reaction amplitudes is severely complicated by the vector character of the meson. It requires the measurement of at least 23 observables. This is more challenging (but also provides more information) than in pseudoscalar meson photoproduction. Similar to other interesting channels, such as double pion photoproduction, the hope is that few polarization observables already provide essential constraints.

A prerequisite to extract resonance information from ω photoproduction is the understanding of the associated reaction dynamics. At high energies, the cross section of vector meson production off nucleons falls off exponentially with the squared recoil momentum, t , corresponding to the range of the mutual interaction. The universal t -dependence of the cross section is characteristic for “diffractive” production. It is associated to the exchange of natural parity quantum numbers (Figure 1 left) related to the Pomeron, a composite gluonic or hadronic struc-

*corresponding author; Electronic address: schmieden@physik.uni-bonn.de

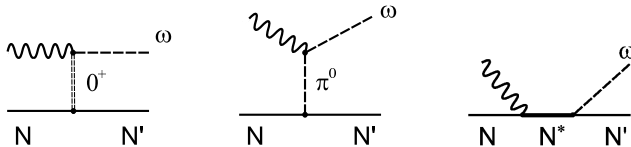


FIG. 1: Contributions to ω photoproduction: natural parity t-channel exchange (left), π^0 t-channel exchange (middle), s-channel intermediate resonance excitation (right).

ture. At large $|t|$ deviations from pure diffraction show up [3]. From the comparison to QCD-inspired models [4] which are also able to describe ϕ and ρ^0 photoproduction, the presence of hard processes in the exchange itself was concluded at $|t| > 1 \text{ GeV}^2$.

Due to the sizeable $\omega \rightarrow \pi^0\gamma$ decay (8%), significant unnatural parity π^0 exchange has been expected for ω -photoproduction at smaller energies (Figure 1 middle). It was indeed observed [5] and found dominating close to threshold [6]. However, neither Pomeron nor π^0 exchange are able to reproduce the strong threshold energy dependence of the cross section and the ω decay angular distribution observed in exclusive photoproduction [7] and electroproduction [8]. This was interpreted as possible evidence for s-channel contributions (Figure 1 right). Complementary experimental support comes from a first measurement of photon beam asymmetries, Σ , through the GRAAL collaboration [9]. Recent coupled-channel analyses yielded however inconclusive results [10, 11].

This provided our motivation to further investigate the reaction $\gamma p \rightarrow p \omega$ with linearly polarized photon beams. We extended the energy range of the previous beam asymmetry measurements and determined for the first time the pion asymmetry Σ_π , which is related to the $\omega \rightarrow \pi^0\gamma$ decay. Σ_π provides new information on the mechanism of ω photoproduction. It is measured in the laboratory frame relative to the photon polarization plane and related to the usual decay asymmetry (in the vector-meson rest frame) by a corresponding Lorentz boost. In the case of a pure π^0 exchange mechanism $\Sigma_\pi \simeq -0.5$ is expected, $+0.5$ for pure Pomeron exchange. The large values of ± 0.5 correspond to fixed parity exchange [12]. If s-channel resonances contribute in a manner compatible with the partial wave decomposition of the available cross section data [12, 13], Σ_π should be close to zero. In contrast, the photon asymmetry Σ is expected to be zero or very close to zero for a pure t-channel mechanism, i.e. pure π^0 exchange, pure Pomeron exchange, and in case of interference of both. It should become large with s-channel resonance contributions [12, 14, 15].

The measurement of the photon-beam asymmetry requires linearly polarized photon beams. The photoproduction cross section off a nucleon can then be cast into the form

$$\frac{d\sigma}{d\Omega} = \frac{d\sigma_0}{d\Omega} (1 - P_\gamma \Sigma \cos 2\Phi), \quad (1)$$

where σ_0 denotes the polarization independent cross sec-

tion, P_γ the degree of linear polarization of the incident photon beam, and Φ the azimuthal orientation of the reaction plane with respect to the plane of linear polarization. The pion asymmetry is obtained if in Eq. 1 the azimuthal angle of the ω meson, Φ , is replaced by the angle Φ_π of the decay- π^0 . This convention gives Σ_π a sign equivalent to Σ , but opposite to the (charged) decay asymmetry as defined in e.g. [16].

The experiment was performed at the tagged photon beam of the ELSA electron accelerator of the University of Bonn. Using electron beams of $E_0 = 3.2 \text{ GeV}$ coherent bremsstrahlung was produced from a $500 \mu\text{m}$ thick diamond crystal. After radiating a photon the electrons were momentum analysed in a magnetic dipole (tagging-) spectrometer, covering a photon energy range of $E_\gamma = 0.18\text{--}0.92E_0$. The photon beam, linearly polarized along the vertical direction, was incident on a 5.3 cm long liquid hydrogen target with $80 \mu\text{m}$ Kapton windows. A three layer scintillating fiber detector [17] surrounded the target within the polar angular range from 15 to 165 degrees. It determined a point-coordinate for charged particles.

Both, charged particles and photons were detected in the **Crystal Barrel** detector [18]. It was cylindrically arranged around the target with 1290 individual CsI(Tl) crystals of 16 radiation lengths in 23 rings, covering a polar angular range of $30 - 168$ degrees. For photons an energy resolution of $\sigma_E/E = 2.5\%/\sqrt{E/\text{GeV}}$ and an angular resolution of $\sigma_{\Theta,\Phi} \simeq 1.1$ degree was obtained.

The $5.8 - 30$ degree forward cone was covered by the TAPS detector [19], set up in one hexagonally shaped wall of 528 BaF₂ modules at a distance of 118.7 cm from the target. For photons between 45 and 790 MeV the energy resolution is $\sigma_E/E = (0.59/\sqrt{E/\text{GeV}} + 1.9)\%$ [20]. The position of photon incidence could be resolved within 20 mm . To discriminate charged particles each TAPS module has a 5 mm plastic scintillator in front of it. The TAPS detectors are individually equipped with photomultiplier readout. The first level trigger was derived from TAPS. A cluster recognition for the **Crystal Barrel** provided a second level trigger.

The ω was identified through its decay into $\pi^0\gamma$. Four detector hits were required during the offline analysis, corresponding to three photons and the proton. Basic kinematic cuts were applied in order to ensure longitudinal and transverse momentum conservation. In the analysis we consider all combinatorial possibilities of the detector hits. For the proton candidate the detected angles directly enter the analysis; the energy information is not used. In addition, it turned out important to *not* positively require proton identification through the signals of the inner scintillating fiber detector of the barrel or the veto detectors of TAPS, in order to reduce the bias from detector inefficiencies on the azimuthal distributions.

Fig. (2) shows the $\pi^0\gamma$ invariant mass distribution for the full photon energy and angular range. The main source of background is $2\pi^0$ production where one of the decay photons escaped detection, either through the

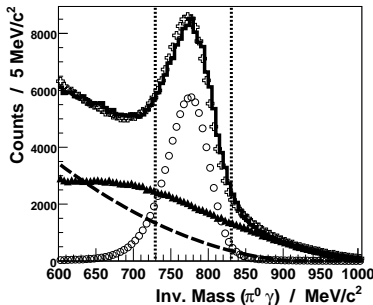


FIG. 2: The $\pi^0\gamma$ invariant mass distribution around the ω signal from the full energy and angular range. The full histogram represents the experimental distribution. Monte Carlo simulations are shown for the ω signal (circles) and the $2\pi^0$ background (triangles). The dashed line is the additional polynomial background (see text), and the crosses show the sum of backgrounds and signal. The mass range accepted in the analysis is indicated by the vertical lines.

(small) detector leaks in extreme forward/backward direction, or because one energy deposit remained below the $\simeq 25$ MeV threshold – in which case the three detected photons practically carry the full kinematic information of the $2\pi^0$ event. Additional non- $2\pi^0$ background was bin-wisely fitted by a polynomial as shown in Fig. 2.

Cuts of ± 50 MeV width around the ω mass were applied in the invariant mass spectra. The photon-beam asymmetry was determined according to Eq. (1). Fits of the azimuthal event distribution in the individual bins of energy and angle were performed (see example in Fig. 3),

$$f(\Phi'_{(\pi)}) = A + B \cos 2\Phi'_{(\pi)}, \quad (2)$$

of both the directions of the reconstructed ω and the decay π^0 with respect to the horizontal lab plane ($\Phi' = \Phi + \frac{\pi}{2}$). The ratio B/A of the fit determines the product of beam(pion) asymmetry and photon polarization, $P_\gamma \Sigma_{(\pi)}$, of Eq. 1. The asymmetries are based on all events within the mass range indicated in Fig. 2. The background can not be subtracted on an event-by-event basis. Instead we corrected the experimental asymmetry according to the fractional background contribution and background asymmetry.

Of particular importance is the $2\pi^0$ background, because the associated events potentially carry sizeable beam asymmetry [21]. Fortunately, in the $\pi^0\gamma$ invariant mass range considered here, the remaining asymmetries turn out relatively small, typically in the range of 10% [22, 23]. For the non- $2\pi^0$ (polynomial) background zero asymmetry was assumed. To estimate the systematic error associated with the subtraction method, the magnitude of the $2\pi^0$ and non- $2\pi^0$ backgrounds were varied from 0–100% (relative) in the fit of the invariant mass distribution. In addition, both background asymmetries were assigned errors of $\delta a \simeq \pm 11\%$ absolute.

The second important source of systematic errors is the angular dependent variation of detector efficiencies. Those may affect the measured Φ distributions in spite of

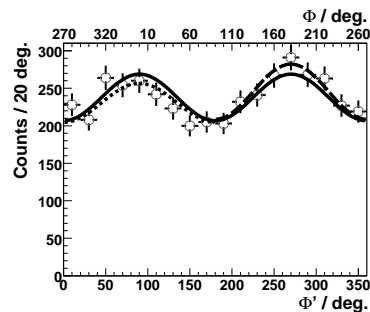


FIG. 3: Azimuthal distribution of the reconstructed ω direction with respect to the plane of photon linear polarization (Φ , top abscissa) and to the horizontal x-axis of the standard laboratory frame (Φ' , bottom abscissa) within the bin $E_\gamma = 1200$ -1300 MeV and $\Theta_{\omega}^{\text{cm}} = 85$ -100 degree. The solid curve represents the full fit. The separate fits of left and right region are denoted dashed and dotted (see text).

the azimuthally symmetric layout of the detector setup. To estimate the associated systematic error, use was made of the fact that, due to the $\cos 2\Phi$ dependence, the azimuthal modulation over the full azimuth carries a twofold redundancy. Any deviation in separate left/right fits (where one example is shown in Fig. 3) in excess of an 1σ statistical fluctuation was assigned to systematics.

The total systematic error varies over the individual bins of energy and angle. In average, $\delta_{\text{syst}} \Sigma = 0.09$ and $\delta_{\text{syst}} \Sigma_\pi = 0.08$ are obtained for Σ and Σ_π , respectively. This also includes the uncertainty in the absolute degree of beam polarization of $\delta P_\gamma < 2\%$ [24] which however is practically negligible.

The main results of our measurements are shown in Figure 4. All energy bins are included in each part of the figure as described in the caption. The left part shows Σ as a function of $|t|$. Unlike the cross section in the diffractive regime the beam asymmetry does not show a universal, i.e. energy independent, $|t|$ -dependence. This is to be expected for a pure kinematic reason. Due to the intrinsic $\sin^2 \Theta_{\text{cm}}$ dependence of Σ , it is forced to zero in each energy bin at the smallest and largest possible $|t|$ which correspond to forward and backward production, respectively. It is however found that Σ exhibits an universal dependence on the ωp center-of-mass angle Θ_{cm} (Fig. 4 middle). This may be associated to intermediate s -channel excitations with specific decay patterns. Also the large magnitude of the beam asymmetries at $\Theta_{\text{cm}} > 80$ degree seems hardly reconcilable with pure t -channel processes [12, 14, 15].

Resonance contributions are further supported by the pion asymmetry Σ_π (Fig. 4 right). In the angular region beyond 80 degree where Σ is large, Σ_π is close to zero as, according to the introductory discussion, may be expected with significant resonance contributions. The Θ_{cm} -dependence appears universal again. In the forward angular region, $\Theta_{\text{cm}} < 80$ degree, Σ_π exhibits larger spreads around 0, consistent with more dominating t -

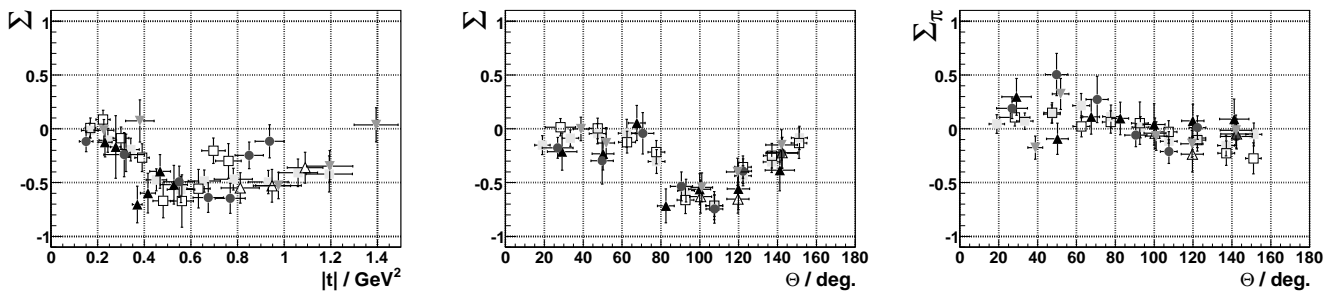


FIG. 4: Photon beam asymmetries and pion asymmetries with total error bars (statistical and systematic errors added in quadrature). In each figure all different energy bins are included: 1108-1200 MeV (full triangles tip up), 1200-1300 MeV (open squares), 1300-1400 MeV (circles), 1400-1500 MeV (open triangles), and 1500-1700 MeV (full triangles tip down). The full squares represent the full energy range. On the *left* Σ is shown as a function of $|t|$, in the *middle* Σ as a function of Θ_{cm} , and on the *right* Σ_{π} as a function of Θ_{cm} .

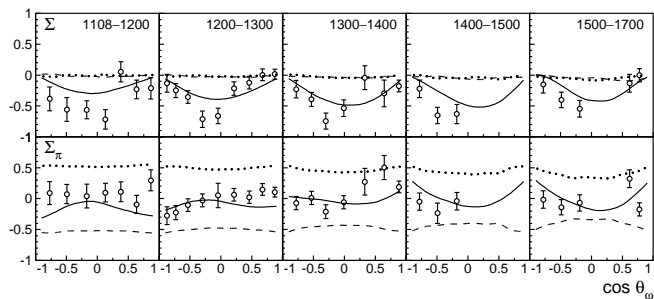


FIG. 5: Comparison of the experimental data for Σ (upper row) and Σ_{π} (lower row) to the Bonn-Gatchina PWA. The PWA uses the experimental binning in E_{γ} from 1108 to 1700 MeV. Three versions of the PWA are shown: pure π^0 -exchange (dashed), pure pomeron exchange (dotted), and the full solution (based on a fit to unpolarized data and the GRAAL beam asymmetry; the experimental data presented here were *not* included).

exchange.

These findings are further corroborated through quantitative comparison of our new data to the Bonn-Gatchina PWA [12, 13] shown in Figure 5. In addition to the pseudoscalar channels, the PWA is based on the

SAPHIR [7] and GRAAL [9] ω photoproduction data. Our new data are *not* incorporated. On top of t -exchange, the PWA allows for resonant partial waves. The far dominant $3/2^+$ one is associated to the $P_{13}(1720)$.

In summary, we have measured beam asymmetries and pion asymmetries in ω -photoproduction off the proton from threshold to $E_{\gamma} = 1700$ MeV using the $\omega \rightarrow \pi^0\gamma$ decay. Large beam asymmetries are observed. Independent of the photon energy those exhibit an universal dependence on Θ_{cm} but not on t . The pion asymmetry is practically zero in the angular range where beam asymmetries are large. These findings indicate significant s -channel contributions, in agreement with the expectation from the Bonn-Gatchina PWA.

We acknowledge very helpful discussions with A. Titov. Outstanding efforts of the ELSA accelerator group enabled the high quality beam. This work was financially supported by the federal state of *North-Rhine Westphalia* and the *Deutsche Forschungsgemeinschaft* within the SFB/TR-16. The Basel group acknowledges support from the *Schweizerischer Nationalfonds*, the KVI group from the *Stichting voor Fundamenteel Onderzoek der Materie* (FOM) and the *Nederlandse Organisatie voor Wetenschappelijk Onderzoek* (NWO).

-
- [1] F. Wilczek, hep-ph/0201222v2.
[2] S. Capstick and W. Roberts, Prog. Part. Nucl. Phys. **45**, 241 (2000).
[3] M. Battaglieri et al., Phys. Rev. Lett. **90**, 022002 (2003).
[4] F. Cano and J. M. Laget, Phys. Rev. D **65**, 074022 (2002).
[5] J. Ballam et al., Phys. Rev. A **7**, 3150 (1973).
[6] B. Friman and M. Soyeur, Nucl. Phys. A **600**, 477 (1996).
[7] J. Barth et al., Eur. Phys. Journal A **18**, 117 (2003).
[8] P. Ambrozewicz et al., Phys. Rev. C **70**, 035203 (2004).
[9] J. Ajaka et al., Phys. Rev. Lett. **96**, 132003 (2006).
[10] G. Penner and U. Mosel, Phys. Rev. C **66**, 055212 (2002).
[11] V. Shklyar et al., Phys. Rev. C **71**, 055206 (2005).
[12] A. Sarantsev et al., arXiv:0806.4477v1.
[13] A. Anisovich et al., Eur. Phys. J. A **25**, 427 (2005).
[14] A. Titov and T.-S. H. Lee, Phys. Rev. C **66**, 015204 (2002).
[15] Q. Zhao et al., Phys. Rev. C **71**, 054004 (2005).
[16] K. Schilling et al., Nucl. Phys. B **15**, 397 (1970).
[17] G. Suft et al., Nucl. Instr. Meth. A **538**, 416 (2005).
[18] E. Aker et al., Nucl. Instr. Meth. A **321**, 69 (1992).
[19] R. Novotny et al., IEEE transaction on nuclear science **38**, 378 (1991).
[20] A. R. Gabler et al., Nucl. Instr. Meth. A **346**, 168 (1994).
[21] V. Sokhoyan, Phd thesis (in preparation), Bonn (2008).
[22] F. Klein, Phd thesis (in preparation), Bonn (2008).
[23] F. Klein et al., to be submitted to EPJA (2008).
[24] D. Elsner et al., Eur. Phys. Journal A **33**, 147 (2007).